Title

Multi-parametric analysis reveals metabolic and vascular effects driving differences in BOLD-based cerebrovascular reactivity associated with a history of sport concussion.

Journal

Brain Injury, 33(11)

Authors

Champagne, Allen

Coverdale, Nicole

Germuska, Michael

et al.

Publication Date

2019

DOI

10.1080/02699052.2019.1644375

Peer reviewed

Published in final edited form as:
Brain Inj. 2019 January 01; 33(11): 1479–1489. doi:10.1080/02699052.2019.1644375.

Multi-parametric analysis reveals metabolic and vascular effects driving differences in BOLD-based cerebrovascular reactivity associated with a history of sport concussion

Allen A. Champagne, PhD[1,*], **Nicole S. Coverdale**[1], **Michael Germuska, PhD**[2], **Douglas J. Cook, MD, PhD**[1,3]

[1]Centre for Neuroscience Studies, Queen's University, Kingston, ON, Canada

[2]Cardiff University Brain Research Imaging Center, Cardiff University, Cardiff, United Kingdom

[3]Department of Surgery, Queen's University, Kingston, ON, Canada

Abstract

Objective—Identify alterations in cerebrovascular reactivity (CVR) based on history of sport-related concussion (SRC). Further explore possible mechanisms underlying differences in vascular physiology using hemodynamic parameters modelled using calibrated magnetic resonance imaging (MRI).

Method—End-tidal targeting and dual-echo MRI were combined to probe hypercapnic and hyperoxic challenges in athletes with (n=32) and without (n=31) a history of SRC. Concurrent blood oxygenation level dependent (BOLD) and arterial spin labelling (ASL) data was used to compute BOLD-CVR, ASL-CVR, and other physiological parameters including resting oxygen extraction fraction (OEF_0) and cerebral blood volume (CBV_0). Multiple linear and logistic regressions were then used to identify dominant parameters driving group-differences in BOLD-CVR.

Results—Robust evidence for elevated BOLD-CVR were found in athletes with SRC history spreading over parts of the cortical hemispheres. Follow-up analyses showed co-localized differences in ASL-CVR (representing modulation of cerebral blood flow) and hemodynamic factors representing static vascular (i.e., CBV_0) and metabolic (i.e., OEF_0) effects suggesting that group-based differences in BOLD-CVR may be driven by a mixed effect from factors with vascular *and* metabolic origins.

[*]**Corresponding Author:** Douglas J. Cook, Department of Surgery, Queen's University Room 232, 18 Stuart St., Kingston, ON K7L 3N6, Phone: 613-549-6666 ext. 3696, Fax: 613-548-1346, dj.cook@queensu.ca. **Other contact information** Allen A. Champagne, Centre for Neuroscience Studies, Room 260, Queen's University, Kingston ON K7L 3N6, a.champagne@queensu.ca, 613-533-6360, Fax: (613) 533-6840; Nicole S. Coverdale, Centre for Neuroscience Studies, Room 260, Queen's University, Kingston ON K7L 3N6, nc68@queensu.ca, 613-533-6360, Fax: (613) 533-6840; Michael Germuska, Cardiff University Brain Research Imaging Centre, School of Psychology, Cardiff University, Maindy Road, Cardiff, CF24 4HQ, germuskam@cardiff.ac.uk, +44 (0) 29 2087 0365, Fax: +44 (0) 29 208 70339.

Author contribution statement

A.A.C and N.S.C. were responsible were the collection of the data. M.G. helped with the computational framework designed for the data analysis. A.A.C. wrote the manuscript and performed all analyses on the data. D.J.C. supervised the project. All authors discussed the results and contributed to editing the final manuscript.

Disclosure/Conflicts of interest

The authors declare no conflict of interest.

Europe PMC Funders Author Manuscripts

Conclusion—These results emphasize that while BOLD-CVR offers promises as a surrogate non-specific biomarker for cerebrovascular health following SRC, multiple hemodynamic parameters can affect its relative measurements.

Keywords

cerebrovascular reactivity; calibrated MRI; sport-related concussion; cerebral blood flow; neuroimaging

1 Introduction

Rate of sport-related concussion (SRC) have increased in recent years due to increased reporting and awareness (1–3). This has raised concerns about the possible long-terms effects of head injuries on brain health. Clinically, SRC is defined as a change in brain function in response to a direct, or indirect, biomechanical insult to the head, which results in physical, cognitive and behavioral symptoms (4). In recent years, neuroimaging research using functional magnetic resonance imaging (fMRI) has focused primarily on studying the acute and sub-acute effects of head injuries (5–9). These studies indicate that neurologic function may be impaired temporarily post-injury, despite no findings on conventional clinical imaging methods such as computed tomography and T_1-weighted MRI imaging (4). This is in concordance with the knowledge that sub-acute impairments in working memory (10,11), neural recruitment (5,12) and cortical network connectivity (13–15) may persist beyond clinical recovery of SRC, which typically occurs between 7-14 days in collegiate athletes (16–18). Emphasis on symptomatic and subacute SRC patients has limited our understanding of the long-term and more chronic consequences of concussion (*see* (19) for review). Examining athletes with a more distant history of concussion may provide additional insight into the mechanisms responsible for impairments in neurocognitive function and development of depression-like symptoms observed in retired professional football athletes (20,21).

Observable changes in brain network connectivity (22) and cerebral blood flow (CBF) (23) associated with a history of concussion have been reported in active collegiate athletes. Together, these changes suggest that the long-term sequalae of concussion could involve disturbances in the neurovascular coupling mechanisms that match CBF with the metabolic needs of the brain during rest and activation. This link between neuronal activity and concomitant regiospecific increases in blood flow is the basis for the blood oxygenation level dependent (BOLD) signal, as a surrogate for changes in neural activation (24). Upon neuronal firing, functional hyperemia to active regions of the brain (25) dilutes local concentrations of deoxy-hemoglobin ([dHb]), which lengthens the T_2* relaxation rates and increases the BOLD signal. Thus, in the setting of altered regulatory processes responsible for modulation of CBF following SRC (26–30), possible injury to the integrity of the vascular system may alter the coupling processes that determine the amplitude of the change in BOLD signal upon exposure to resting- or task-based paradigms.

Techniques combining respiratory end-tidal targeting and fMRI have allowed probing of the vasodilatory response in the arteriolar vessels, independently of functional tasks (31–33).

Europe PMC Funders Author Manuscripts

This is done by increasing the arterial partial pressure of carbon dioxide (P_aCO_2), which results in global pH changes that are counteracted by increases in blood flow (25,34). The magnitude of the changes in CBF following hypercapnia (HC) normalized to the change in end-tidal CO_2 ($P_{ET}CO_2$) is known as cerebrovascular reactivity (CVR). Thus, assuming that the cerebral metabolic rate of oxygen consumption ($CMRO_2$) remains constant during HC (35), CVR can be used as a tool to interrogate the integrity of the brain's regulatory processes responsible for control of CBF.

Calibrated fMRI methods allow us to relate an observed BOLD signal change to an underlying change in CBF scaled by the maximum possible BOLD signal, M. Thus, it is clear that the BOLD-CVR response maybe altered either by a change in the CBF response to a stimulus, or by a change in the maximum BOLD signal. Knowledge of these underlying physiological processes can elucidate co-localized differences in physiological markers that modulate differences in BOLD fMRI (36–38) observed in clinical populations (39–41).

In this study, we use BOLD-CVR to investigate the long-term effects of SRC on vascular reactivity in collegiate football players, providing insight into the lasting effects of SRC on vascular health. The interaction between history of SRC and position played was also investigated as an indirect way to assess the effects of cumulative non-symptomatic head trauma on brain physiology. This is relevant given that repetitive exposure to sub-concussive head impacts differs across football positions (42–45) and that such exposure may also be associated with chronic imaging findings in retired players (46). In addition to BOLD-CVR, we simultaneously acquired complementary physiological parameters, including changes in CBF (acquired using concurrent arterial spin labelling (ASL)), and metabolic and static vascular parameters derived from physiological models of calibrated fMRI signal changes (38–43), to explore possible mechanisms underlying differences in BOLD-CVR. These measurements, along with further parametrization of M in terms of resting venous blood volume (CBV_0) and venous oxygenation (γ_v), via Equation (1), can be used to assess the physiological parameters that are combined to make up the BOLD response.

$$M = A \cdot TE \cdot CBV_0 \cdot B^{\beta} \cdot (1 - \gamma_v)^{\beta}. \quad \text{Eq. (1)}$$

We hypothesized that there would be group-differences in BOLD-CVR, associated with history of SRC. Furthermore, we predicted that group-differences in BOLD-CVR would be driven most strongly by direct changes in CBF during HC (ASL-CVR), given the linear relationship between BOLD and changes in CBF (37).

2 Methods

2.1 Subjects and ethical approval

The experimental protocol used in this study was approved by the Queen's University Health Sciences Research Ethics Board (Kingston, ON, Canada) and informed consent was signed for all participants. In this study, a total of 63 current male collegiate football athletes with and without history of SRC were recruited to participate in the MRI protocol (Table 1). Of those, 32 (mean age = 19 ± 3 years) reported a previous history of concussion ("HX";

Europe PMC Funders Author Manuscripts

range = [1,4]) and 31 age-matched athletes reported no history of head injury ("CTL"). The subject's height, weight and concussion history were collected through a demographic questionnaire filled out by the athlete prior to the MRI.

2.2 Experimental protocol

2.2.1 Assessment of symptomology—Prior to completing the MRI protocol, all participants were asked to complete the symptom evaluation section from the Sport-Concussion Assessment tool (3rd edition; SCAT (47)), in order to assess whether long-term symptoms related to SRC were persistent in the HX group.

2.2.2 Hypercapnia and hyperoxia breathing paradigm—Each protocol included two 6 minutes functional MRI acquisitions collected separately: one HC and one hyperoxia (HO). A feed-forward gas delivery system (RA-MR™, Thornhill Research Inc., Toronto, Canada) and breathing circuit (48) were used to target prospective CO_2 and O_2 ($P_{ET}O_2$) end-tidal values while the participants were in the MRI. Each breathing paradigm consisted of a 2-minute baseline, a 2-minute breathing step, and a 2-minute recovery period (Figure 1). HC was targeted at 10 mmHg above the subject's resting parameters, and HO was targeted at 410 mmHg. Constant normoxia (~110 mmHg) and normocapnia were maintained during the HC and HO challenges, respectively. This was done to limit the vasoconstricting effects of increased $P_{ET}O_2$ during HC (49) and the confounding vasodilatory effects of elevated $P_{ET}C_{O2}$ on CBF during HO (50,51).

Prior to the MRI protocol, subjects were instructed to pace their breathing to a breathing metronome delivered using both visual and auditory stimulus generated in PsychoPy (Version 2.0, University of Nottingham) (52,53) to maintain their respiratory rate at ~12 breaths/min. The participants' resting parameters were acquired during the anatomical scan (see below) while the subjects breathed to the metronome.

2.2.3 Magnetic resonance imaging protocol—All images were acquired on a Siemens 3.0T Magnetom Tim Trio system using a 32-channel receiver head coil. First, a whole-brain anatomical T_1-weighted MPRAGE (Magnetization Prepared Rapid Acquisition Gradient Echo) sequence was completed and used for proper tissue segmentation and registration. The following parameters were used: TR = 1760ms, TE = 2.2ms, time of inversion (TI) = 900ms, voxel size = 1mm isotropic, field of view (FOV) = 256 x 256mm, flip angle = 9°, receiver bandwidth = 200 Hz/pixel, for a total scan time of 7 minutes and 32 seconds.

During each breathing manipulation, concordant BOLD and CBF data were acquired using a dual-echo pseudo-continuous arterial spin labelling sequence (pCASL) (54). An echo planar imaging (EPI) readout was used with the following parameters: TR = 4000ms, TE_1/TE_2 = 10/30ms, FOV = 250 x 250mm, flip angle = 90°, voxel size = 3.9mm isotropic, nominal post-labeling delay (PLD) = 1000ms, slice gap = 0.773mm, label offset = 100mm, receiver bandwidth = 2604 Hz/pixel, EPI factor = 64, tagging duration 1.665s (55). The whole brain was captured using a total of 25 axial slices acquired in an ascending manner on a 64x64 matrix (7/8 Partial Fourier) with parallel imaging (GRAPPA acceleration factor = 2). An additional tissue magnetization map (M_0) was acquired for CBF quantification during the

break period between the HC and HO protocols (Figure 1). The same pCASL parameters were used for the M_0 scan, with a longer TR (15,000ms) to allow for full relaxation of the tissues, and no spin labelling (static signal only). All EPI images were pre-normalized using the body transmit/receiver coil in order to correct for inhomogeneities in the receive sensitivity of the 32-channel head coil.

2.3 Data preprocessing

All datasets acquired in this study were preprocessed using combined scripts from FSL (56), AFNI (57), and Matlab (MATLAB 2015b, The MathWorks, Inc., Natick, Massachusetts, United States). The pCASL data from both HC and HO were first brain extracted using the brain extraction tool (*BET*), followed by motion correction (*MCFLIRT;* (58,59)) based on the $(n+1)^{th}$ volume of the timeseries. Once re-aligned, HC, HO and M_0 scans were co-registered into each subject's native space using FSL's *epi_reg* tool (56) and *topup* (60,61) to simultaneously correct for subject movement and susceptibility induced distortions.

BOLD and ASL timeseries were extracted individually from the pCASL data (54). BOLD images were reconstructed using a surround averaging method of the second echo (TE = 30ms) in order to maximize SNR (62). The BOLD data were then smoothed using a Gaussian kernel of 8mm with FSL's *SUSAN* tool (56) and high-pass filtered at 0.003 Hz to remove any linear drift from the EPI acquisition (56). CBF data were reconstructed using a linear surround subtraction between the control and tag frames from the ASL timeseries (TE = 10ms) and spatially smoothed. Following *despiking* of the signal (57), the perfusion data were converted to physiological units using the single-blood compartment model (Eq. (2)) (63):

$$CBF = \frac{6000\lambda \cdot \Delta M \cdot R_{1b}}{2\alpha_{inv} \cdot M_0 \cdot (e^{-PLD \cdot R_{1b}} - e^{-(\tau + PLD) \cdot R_{1b})}} \cdot \left[\frac{\frac{ml}{100g}}{min}\right], \quad \text{Eq. (2)}$$

and the following parameters: blood/tissue water partition coefficient (λ) = 0.9ml/g (64), labelling duration (τ) = 1.665s, and arterial blood longitudinal relaxation rate ($R_{1b} = 1/T_{1b}$) = 1/1.650s (65), as well as a linear slice-by-slice correction of the PLD values to account for the ascending axial 2D EPI readout. The inversion efficiency (α_{inv}) was set to 0.84 for baseline and HO volumes, and 0.80 for the HC images to account for increasing flow velocity during HC (66). Per-volume adjustments for the vasoconstrictive effects of HO on CBF (49) were also modelled into the calibration using (67) (*Appendix A.1.2*), and the linear relationship between R_1 and PaO_2 (68).

2.4 Estimation of cerebrovascular reactivity

Grey-matter tissues were segmented automatically from the high-resolution T_1-weighted MPRAGE image using *FAST* (69), and re-sampled into low-resolution native space (isometric 3.9 mm). A voxel-based general linear model was then computed using the $P_{ET}CO_2$ and $P_{ET}O_2$ traces for HC and HO respectively. Parameters were converted to Z statistics thresholded at $-2.3 > Z > 2.3$ and the conjunction between supra-threshold voxels and grey-matter tissues were used to define the subject's functional region of interest (ROI) where the signal was significantly modulated by the breathing manipulations.

Pre-processed volumes acquired during baseline and stimulus periods were averaged to create mean baseline, hypercapnic and hyperoxic BOLD and CBF images. In order to avoid biases from temporal delays in the vascular response to HC (70–73), the final 80 s period of the block was used to compute the stimulus mean images. BOLD- and ASL-based CVR maps were calculated as the percent change in BOLD and CBF from baseline, divided by the magnitude change in $P_{ET}CO_2$ recorded during hypercapnia ($CVR = \%\Delta Signal / \Delta P_{ET}CO_2$).

2.5 Computation of M, OEF_0 and CBV_0 voxelwise maps

Concurrent changes in BOLD and CBF during HC and HO were used to model the voxelwise M parameter and resting oxygen extraction fraction (OEF_0) maps simultaneously (Figure 2), for each subject, based on the original biophysical model proposed by (74) and (37), and the dual-calibration method described in (75,76). In this model (76) (**see** Equation (1)), the theoretical M relates changes in BOLD to fractional changes in [dHb] ($[dHb]/[dHb]_0$). Additionally, CBV/CBV_0 is estimated by way of the non-linear coupling between flow and venous volume during HC and HO using $(CBF/CBF_0)^{\alpha}$, where the Grubb coefficient (α) was set to 0.18 (35). The $[dHb]/[dHb]_0$ was modeled based on a function that relates changes in arterial oxygen content (C_aO_2), and fluctuations in flow during both breathing manipulations, described in (76) (***see*** Equation (2)). All modelling parameters were consistent with the original method (76) and $CMRO_2$ was assumed to remain constant (iso-metabolism; $CMRO_2/CMRO_{2/0} = 1$) during each breathing paradigm (35). The parameter β, representing the non-linear coupling between changes in [dHb] and R_2*, was set to 1.3, which is appropriate for a field strength of 3.0T (77).

Venous CBV_0 maps (Figure 2) were computed using the BOLD HO data and the analytical model proposed by (78) (***see*** Equation 11). This approach was shown to reduce uncertainty associated with variations in baseline physiology, compared to previous methods proposed for measuring venous CBV non-invasively (79).

2.6 Data analysis

2.6.1 Voxelwise analysis of BOLD-CVR maps—

Prior to group-based analysis, the participants' T_1-weighted images were spatially transformed into MNI standard space (2mm isotropic) using affine (12 dof; (58)) and non-linear warp-fields (*FNIRT;* (80)). These transformation matrices were concatenated with linear parameters from native to anatomical space registration, and then used to warp BOLD-CVR into MNI space.

Voxel-based group comparison on individual BOLD-CVR maps were performed in AFNI (57) using an ANCOVA with *3dMVM* (81). The subjects' age, height, weight and baseline $P_{ET}CO_2$ values were all included as covariates in the statistical model. Significant clusters were identified using a height threshold of $P < 0.05$ and a cluster volume > 602 voxels, corrected for family-wise error from multiple comparisons based on Monte Carlo stimulations (10,000 iterations) in AFNI's *3dClustSim* (82,83).

2.6.2 Parametrization and post-hoc analysis of physiological parameters—

Statistically significant regional clusters were binarized to create a region of interest (ROI) for *post-hoc* analysis. A total of four parameters were extracted in parallel (Table 2), in order

to determine which physiological variables were related to the group-differences in BOLD-CVR. M was further broken down into its constituent parts, based on Eq. (1). Here, we let OEF_0 equal $(1 - \gamma_v)$ as an approximation for the baseline metabolic effects on M (and BOLD). κ was set to $\frac{M}{CBV_0 \cdot OEF_0^{\beta}}$ (**Eq.(3)**) to represent a lumped parameter for [Hb], vessel size and morphology, and intra- and extra-vascular effects on the BOLD signal (74,84).

Mean measurements were extracted for each parameter and imported into IBM SPSS statistics (version 24.0, SPSS Inc., Chicago, IL, USA), for further statistical analysis. A significance threshold of $P < 0.05$ was used for the ANCOVA on regional ASL-CVR and M between the CTL and HX groups. Multiple linear and logistic regressions were then used to classify group differences in BOLD-CVR using the proposed parametrization in Table 2, and identify dominant parameters driving BOLD-based measurements of vascular reactivity.

Lastly, the relationship between findings in BOLD-CVR and clinical parameters including time since last concussion (years), total number of concussions experienced, and SCAT symptom and severity scores was explored for the HX group using linear regressions and a significance threshold set at $P < 0.05$.

2.6.3 Exploring the effect of position played—

In order to explore the effect of position played on the analysis of BOLD-CVR between the groups, both CTL and HX groups were further split into three position groups based on typical exposure to head impacts in collegiate football players (44,45): BIG (defensive and offensive linemen), BIG-SKILL (full backs, linebackers, running backs, tight-ends), and SKILL (defensive backs, kickers, quarterbacks, safeties, wide-receivers). These subgroups were then used to assess the interaction between concussion history and position played on mean ROI BOLD-CVR values. Prior to this sub-analysis, a chi-squared test was conducted to see if there was a significant difference in the distribution of position between the CTL and HX groups.

3 Results

3.1 Participants demographics

There were no differences in age, weight or height between groups ($P > 0.05$; Table 1). There was a significant difference between the groups for concussion history, with HX subjects having sustained their most recent injury 3.46 ± 2.70 years prior to participating in the imaging protocol, on average (Table 1). Additionally, HX reported a greater number and severity of symptoms on the SCAT assessment (Table 1). For position played, 10 BIG, 9 BIG-SKILL and 12 SKILL players made up the CTL group, while the HX group consisted of 8 BIG, 14 BIG-SKILL and 10 SKILL athletes. No significant difference in the distribution of position between the groups was documented based on the chi-squared test ($\chi^2 = 1.798$; $P = 0.407$).

3.2 Respiratory manipulations

The RA-MR™ apparatus reliably targeted of $P_{ET}CO_2$ and $P_{ET}O_2$ during both the HC and HO task (Figure 1). No significant differences in baseline $P_{ET}CO_2$ and $P_{ET}O_2$ were observed between the groups (Table 3). Furthermore, there were no significant differences in the

magnitude of change in CO_2 ($\Delta P_{ET}CO_2$) and O_2 ($\Delta P_{ET}O_2$) in either task (Table 3), confirming that subjects from both groups experienced similar HC and HO challenges, while maintaining normoxia and normocapnia, respectively.

3.3 Differences in BOLD-based CVR and co-localized hemodynamic parameters

Voxelwise group analysis showed significantly higher BOLD-CVR (Table 4; $P < 0.05$, corrected) within the HX group spreading over parts of the right visual cortex, the left superior and inferior parietal lobules, the left premotor motor cortex, the right supplementary cortex, and the right parietal operculum (85) (Figure 3).

Follow-up ROI analysis performed using the significant voxels highlighted in Figure 3 (P<0.00001; CTL=0.21±0.03 %ΔBOLD/mmHg; HX=0.28±0.06 %ΔBOLD/mmHg) showed significant group differences in ASL-CVR (P = 0.014; CTL = 6.01 ± 1.05 %ΔCBF/mmHg; HX = 6.81 ± 1.52 %ΔCBF/mmHg), and M (P = 0.022; CTL = 4.85 ± 1.45 %ΔBOLD; HX = 5.79 ± 1.44 %ΔBOLD), based on SRC history (Figure 4).

Linear regressions showed that parameters from Table 2, along with age (39), explained up to ~62% (P<0.00001) of the variance for BOLD-CVR written as:

$$CVR(BOLD) = constant + 0.5\boldsymbol{CVR_{ASL}} + 0.9\boldsymbol{CBV_0} + 1.3\boldsymbol{OEF_0} + 1.0\boldsymbol{\kappa} + 0.3age\,. \quad \text{Eq. (4)}$$

Logistic regressions indicated that regional BOLD-CVR alone could classify the groups based on SRC history at a success rate of 74%, while the multi-parametric approach using the proposed parameters in parallel improved the classification results up to 79%. More importantly, the same parameters driving the variance in BOLD-CVR (Eq. (4)) were also driving the group differences identified in the ROI, based on standardized beta coefficients computed from the logistic regressions (Table 5).

In an additional analysis, we repeated the ROI analysis for BOLD-CVR using the position groups described in section 2.6.3 to look at the possible interaction effect between position played and SRC history. No significant main effect ($P_{\text{BOLD CVR}}$ = 0.653) or interaction with SRC history ($P_{\text{BOLD CVR}}$ = 0.251) was identified for position played in this sample.

3.4 Relationship between BOLD-CVR findings and clinical factors

ROI measurements for BOLD-CVR showed no significant relationship with the total number of concussions reported (r = 0.058, P = 0.758), the time since last injury (r = 0.303, P = 0.097), the SCAT symptom score (r = 0.179, P = 0.353) and the SCAT severity score (r = 0.205, P = 0.286) for the HX group.

4 Discussion

4.1 Main findings

Our findings indicate that widespread differences in BOLD-CVR may be associated with a history of SRC in collegiate football players. By exploring the region of interest where BOLD-CVR was different in more depth, we demonstrated that BOLD-CVR was a non-

Europe PMC Funders Author Manuscripts

specific marker for both vascular and metabolic changes that may occur regionally, following SRC. More specifically, our findings show that BOLD-based differences in CVR between the groups were primarily driven by resting metabolic factors, via OEF_0, and not ASL-CVR, as originally hypothesized. Thus, proper interpretation of BOLD-CVR results requires a multi-parametric approach, such as the one proposed here, where hemodynamic modulators of BOLD-CVR can all be assessed in parallel. Despite these group differences however, we found no interaction between position played and SRC history, suggesting that repetitive sub-concussive impacts sustained throughout a player's career does not have an impact on BOLD-CVR, while sustaining one or multiple clinically diagnosable SRC may be sufficient to alter cerebrovascular physiology over time.

4.2 Neurovascular factors and BOLD-CVR differences between the groups

In this study, we found elevated BOLD-CVR in collegiate football athletes with a history of SRC. Long-term alterations in CVR may be associated with direct mechanical disruption and injury of the brain tissues, at the arteriolar level, which may result from the strain and shearing forces transferred to the brain upon the injurious impact (primary injury) (86). Differences in vascular physiology may also be associated with secondary injury mechanisms such as mild tissue edema, microcellular injury, and possible neurological deterioration, due to cellular, metabolic and inflammatory processes post-injury (86–88). Despite differences in BOLD-CVR based on history of SRC, no direct relationship with clinical factors such as time since last injury (years) or SCAT scores was documented within the HX group suggesting that the relationship between imaging findings and clinical factors is not linear.

We observed higher ASL-CVR co-localized with increased BOLD-CVR, suggesting that hypersensitive vessels may explain, in part, the greater magnitude of change in the BOLD signal, upon exposure to hypercapnia. This builds on previous observations of the linear relationship between BOLD-CVR and changes in CBF, defining the basis for neurovascular coupling (37). Upon onset of a vasoactive stimulus (e.g. hypercapnia), increases in flow in the larger vessels will feed into the vascular beds (i.e. capillaries), which are perfused in parallel. In healthy tissues, assuming a similar arrival time for that vascular region (70,73), such a stimulus would create a balanced reduction in vascular tone, resulting in increased CBF equally across the capillary beds. In the presence of differences in basal vascular tension between downstream branches however (89), or vasodilatory capacity, direct competition for limited flow may result in a disproportional distribution of the oxygenated blood across vascular beds where the cerebrovascular vasodilatory reserve may be different (reviewed in (86)). Differences in vasodilatory capacity between neighboring vascular beds raises questions about the chronic effects of such physiological mechanisms over time, as these differences would also likely impact the hyperemic response during neural activation, when the local demands for CBF are increased (33). Differences in regulation of arteriolar resistance (90) may also provide mechanisms for more chronic consequences observed in athletes with a history of SRC such as cortical thinning (91) and neurocognitive impairments (21).

In this study, observed differences in M were concurrent with group-differences in BOLD- and ASL-CVR, suggesting that both vascular and hemodynamic factors may underlie local differences in BOLD-CVR. Thus, further parametrization of the M parameter is useful for meaningful interpretation of these results from BOLD-CVR. In contrary to our original predictions, results from the logistic regression show that group-differences in BOLD-CVR may actually be driven most strongly by physiological differences in baseline metabolism, via OEF_0. This is an important finding highlighting the importance of multi-parametric analyses in studying the effects of head injuries on brain physiology, in order to prevent naive interpretation of BOLD-CVR. Differences across the standardized coefficients studied in parallel (Table 5) show that other hemodynamic variables including CBV_0 and κ also influenced the BOLD response to hypercapnia. This is supported by previous work on BOLD fMRI (92) showing that despite finding no direct correlation between $\frac{\Delta CBF}{CBF_0}$ and Y_v, both parameters can account for the majority of the total variance in the BOLD signal. Thus, findings from Liu *et al.* 2013 and this study suggest that the effect of each parameter on the BOLD signal may be achieved through different mechanisms, where static vascular and metabolic effects including CBV_0, OEF_0 and κ modulate M, and dynamic vascular effects from CBF modulation determine ASL-CVR, in ways that they can influence the BOLD signal interdependently.

Using the parametrization proposed above, group classification was improved from ~74 to 79%, suggesting that a multi-parametric approach may provide more information about the alterations in cerebral physiology post-SRC. Potential reasons for long-term differences in CBF modulation, and baseline oxygenation, following SRC, will require additional research, as we continue to advance our understanding of head injuries. However, recent preliminary findings about possible differences in resting metabolism following SRC [*Champagne et al. Under revision*], along with patient-specific alterations in vascular reactivity (26,28,29,93), may provide evidence for early onset alterations in hemodynamic factors, which could persist long beyond clinical recovery of SRC.

4.3 Limitations

This study explored the effects of self-reported SRC on vascular and metabolic parameters underlying changes in BOLD-CVR. An important assumption made in this analysis was that self-reported SRC by the HX subjects was accurate (94). The reliance of this study on self-reported injury history and symptoms should be acknowledged however, as athletes may fail to report previous injuries (95,96).

The parametrization proposed in this study broke down the BOLD-CVR signal into its constituent parts, while assuming values of 0.18 and 1.3 for α and β, respectively. The M parameter was divided by the product of CBV_0 and $OEF_0{}^{\beta}$ (**Eq. (3)**), in order to remove the effect of each variable, and compute κ, which is dependent on [Hb], vessel size and morphology, and intra- and extra-vascular effects. However, these assumptions for α and β limit the accuracy of the coefficients reported for each parameter because they approximate a non-linear relationship between $\frac{\Delta CBF}{CBF_0}$ and the BOLD signal change (84). This also limits our ability to completely separate the effects of OEF_0 from M, and thus κ. Therefore,

coefficients documented in **Eq. (3)** and Table 5 may differ upon better approximation for α and β, in each subject.

The generalizability of the findings from this study is limited by the fact that this analysis did not include females or athletes from other contact and non-contact sports. As well, we were unable to control for lifetime exposure to sub-concussive impacts sustained by football players over the span of an entire career, which may have confounded our results. Although no main effect or interaction with position played was found in this study, the data segregation used in this design was limited in providing an accurate index for each player's lifetime cumulative exposure to sub-concussive microtrauma (44). This could be partially addressed in future research designs using questionnaire such as the one used in (46).

Another limitation of this study is the lack of imaging markers for the neurovascular coupling processes during neural activity, which limits the clinical applications associated with BOLD-based differences in CVR in this sample. In the future, it may be useful to consider using a functional task similar to (97) or (98) to provide complementary evidence for potential differences in task evoked BOLD activation following SRC, and further establish the link between differences in CVR, and possible changes in the coupling mechanisms responsible for CBF modulation during neural activation.

4.4 Conclusion

In this study, we identified robust differences in BOLD-CVR across the brain which were explained, in part, by hemodynamic parameters relating to CBF modulation, and resting metabolic and vascular physiology. These results emphasize that while BOLD-CVR has been used as a surrogate non-specific biomarker for cerebrovascular health following sport-concussion, multiple hemodynamic parameters can affect its relative measurements. Furthermore, these findings highlight that resting metabolic demand, along with coupling mechanisms responsible for regulation of CBF, may confound analyses of BOLD-based fMRI, which is used to probe differences in neuronal recruitment post-SRC. Thus, multi-parametric approaches like the one proposed here should be considered so that CVR analyses, and other BOLD-based imaging designs, can be used as novel tools to characterize the long-term consequences of SRC on brain physiology and function.

Acknowledgements

The authors of this paper would like to thank Mr. Don Brien and Mrs. Janet Mirtle-Stroman for their dedication and willingness to help with data collection. The authors would like to acknowledge Dr. Clarisse I. Mark for her help with collecting parts of the data, along with the Queen's football program (Kingston, Ontario), for their generous contributions and participation in this research project. Finally, we would like to thank Dr. J. J. Wang at UCLA for sharing the pCASL sequence used in this study.

Funding

This work was supported by the Southeastern Ontario Academic Medical Organization (SEAMO). M.G. was supported by Wellcome Strategic Award, ‘Multi-scale and multi-modal assessment of coupling in the healthy and diseased brain’, grant reference 104943/Z/14/Z.

Europe PMC Funders Author Manuscripts

List of Abbreviations

[dHb]	concentration of deoxyhemoglobin
AFNI	Analysis of Functional NeuroImages (https://afni.nimh.nih.gov)
ASL	arterial spin labelling
BIG	position group: defensive and offensive linemen
BIG-SKILL	position group: full backs, linebackers, running backs, tight-ends
BOLD	blood oxygen level dependent
CBF	cerebral blood flow
CMRO2	cerebral metabolic rate of oxygen consumption
CTL	group of control subjects
CVR	cerebrovascular reactivity
fMRI	functional magnetic resonance imaging
FSL	FMRIB software library (https://fsl.fmrib.ox.ac.uk/fsl/fslwiki/)
HC	hypercapnia
HO	hyperoxia
HX	group with history of concussion
M	maximal theoretical BOLD signal upon complete removal of venous dHb
$\mathbf{p^{CASL}}$	pseudo-continuous arterial spin labelling
$\mathbf{P_{ET}CO_2}$	end-tidal carbon dioxide
$\mathbf{P_{ET}O_2}$	end-tidal oxygen
SCAT	sport-concussion assessment tool
SKILL	position group: defensive backs, kickers, quarterbacks, safeties, wide-receivers
SRC	sport-related concussion

References

1. Marar M, McIlvain NM, Fields SK, Comstock RD. Epidemiology of concussions among United States high school athletes in 20 sports. Am J Sports Med. 2012 Apr 1; 40(4):747–55.cited 2016 Feb 22 [PubMed: 22287642]
2. Marshall SW, Guskiewicz KM, Shankar V, McCrea M, Cantu RC. Epidemiology of sports-related concussion in seven US high school and collegiate sports. Inj Epidemiol. 2015; 2(1):13. [PubMed: 27747745]

3. Daneshvar D, Nowinski C. The epidemiology of sport-related concussion. Clin Sport Med. 2011; 30(1):1–17.
4. McCrory P, Meeuwisse WH, Aubry M, Cantu RC, Dvorák J, Echemendia RJ, et al. Consensus Statement on Concussion in Sport-The 4th International Conference on Concussion in Sport Held in Zurich, November 2012. PM R. 2013; 5(4):255–79. [PubMed: 23466418]
5. Hammeke, Ta; McCrea, M; Coats, SM; Verber, MD; Durgerian, S; Flora, K; , et al. Acute and Subacute Changes in Neural Activation during the Recovery from Sport-Related Concussion. J Int Neuropsychol Soc. 2013:1–10.
6. Johnson B, Zhang K, Gay M, Horovitz S, Hallett M, Sebastianelli W, et al. Alteration of brain default network in subacute phase of injury in concussed individuals: Resting-state fMRI study. Neuroimage. 2012; 59(1):511–8. [PubMed: 21846504]
7. Borich M, Babul A-N, Yuan PH, Boyd L, Virji-Babul N. Alterations in Resting-State Brain Networks in Concussed Adolescent Athletes. J Neurotrauma. 2015; 32(4):265–71. DOI: 10.1089/neu.2013.3269 [PubMed: 25010041]
8. Wang Y, Nencka AS, Meier TB, Guskiewicz K, Mihalik JP, Brooks MA, et al. Cerebral blood flow in acute concussion : preliminary ASL findings from the NCAA-DoD CARE consortium. 2018
9. Wang Y, Nelson LD, LaRoche AA, Pfaller AY, Nencka AS, Koch KM, et al. Cerebral Blood Flow Alterations in Acute Sport-Related Concussion. J Neurotrauma. 2016; 33(13):1227–36. DOI: 10.1089/neu.2015.4072 [PubMed: 26414315]
10. Keightley ML, Saluja RS, Chen J-K, Gagnon I, Leonard G, Petrides M, et al. A functional magnetic resonance imaging study of working memory in youth after sports-related concussion: is it still working? J Neurotrauma. 2014; 31(5):437–51. [PubMed: 24070614]
11. Pardini JE, Pardini Da, Becker JT, Dunfee KL, Eddy WF, Lovell MR, et al. Postconcussive symptoms are associated with compensatory cortical recruitment during a working memory task. Neurosurgery. 2010; 67(4):1020–7. [PubMed: 20881565]
12. Howell D, Osternig L, Van Donkelaar P, Mayr U, Chou LS. Effects of concussion on attention and executive function in adolescents. Med Sci Sports Exerc. 2013; 45(6):1030–7. [PubMed: 23274602]
13. Czerniak SM, Sikoglu EM, Liso Navarro AA, McCafferty J, Eisenstock J, Stevenson JH, et al. A resting state functional magnetic resonance imaging study of concussion in collegiate athletes. Brain Imaging Behav. 2015; 9(2):323–32. [PubMed: 25112544]
14. Meier TB, Bellgowan PSF, Mayer AR. Longitudinal assessment of local and global functional connectivity following sports-related concussion. Brain Imaging Behav. 2016; doi: 10.1007/s11682-016-9520-y
15. Borich M, Babul A-N, Huang PH, Boyd L, Virji-Babul N. Alterations in resting state brain networks in concussed adolescent athletes. J Neurotrauma. 2014; 271:1–26.
16. Mccrea M, Guskiewicz KM, Marshall SW, Barr W, Randolph C, Cantu RC, et al. Acute Effects and Recovery Time Following Concussion in Collegiate Football Players. J Am Med Assoc. 2003; 290(19):2556–63.
17. McCrea M, Kelly JP, Randolph C, Cisler R, Berger L, Marshall LF, et al. Immediate neurocognitive effects of concussion. Neurosurgery. 2002; 50(5):1032–42. [PubMed: 11950406]
18. Nelson LD, Guskiewicz KM, Barr WB, Hammeke TA, Randolph C, Ahn KW, et al. Age Differences in Recovery After Sport-Related Concussion: A Comparison of High School and Collegiate Athletes. 2016; 51(2):142–52.
19. Eierud C, Craddock RC, Fletcher S, Aulakh M, King-Casas B, Kuehl D, et al. Neuroimaging after mild traumatic brain injury: Review and meta-analysis. NeuroImage Clin. 2014; 4:283–94. DOI: 10.1016/j.nicl.2013.12.009 [PubMed: 25061565]
20. Guskiewicz KM, Marshall SW, Bailes J, McCrea M, Cantu RC, Randolph C, et al. Association between recurrent concussion and late-life cognitive impairment in retired professional football players. Neurosurgery. 2005; 57(4):719–26. [PubMed: 16239884]
21. Guskiewicz KM, Marshall SW, Bailes J, Mccrea M, Harding HP, Matthews A, et al. Recurrent concussion and risk of depression in retired professional football players. Med Sci Sports Exerc. 2007; 39(6):903–9. [PubMed: 17545878]

22. Churchill N, Hutchison MG, Leung G, Graham S, Schweizer TA. Changes in functional connectivity of the brain associated with a history of sport concussion: A preliminary investigation. Brain Inj. 2017; 31(1):39–48. [PubMed: 27901587]
23. Churchill N, Hutchison M, Richards D, Leugn G, Graham S, Schweizer T. Brain structure and function associated with a history of sport concussion: a multi-modal MRI study. J Neurotrauma. 2016; (416):1–29.
24. Ogawa S, Lee TM, Kay AR, Tank DW. Brain magnetic resonance imaging with contrast dependent on blood oxygenation. Proc Natl Acad Sci U S A. 1990; 87(24):9868–72. [PubMed: 2124706]
25. Attwell D, Buchan AM, Charpak S, Lauritzen M, MacVicar BA, Newman EA. Glial and neuronal control of brain blood flow. Nature. 2010; 468:232–43. [PubMed: 21068832]
26. Len TK, Neary JP, Asmundson GJG, Candow DG, Goodman DG, Bjornson B, et al. Serial monitoring of CO2 reactivity following sport concussion using hypocapnia and hypercapnia. Brain Inj. 2013; 27(3):346–53. [PubMed: 23438354]
27. Mutch WAC, Ellis MJ, Ryner LN. Longitudinal Brain Magnetic Resonance Imaging CO 2 Stress Testing in Individual Adolescent Sports-Related Concussion Patients: A Pilot Study. 2016; 7(July):1–8.
28. Mutch WAC, Ellis MJ, Ryner LN, McDonald PJ, Morissette MP, Pries P, et al. Patient-specic alterations in cO2 cerebrovascular responsiveness in acute and sub-acute sports-related concussion. Front Neurol. 2018; 9(23)
29. Mutch W, Ellis AC, Ryner MJ, Graham LN, Dufault R, Gregson B, et al. Brain magnetic resonance imaging CO2 stress testing in adolescent post-concussion syndrome: pCASL findings. J Neurosurg. 2016
30. Len TK, Neary JP, Asmundson GJG, Goodman DG, Bjornson B, Bhambhani YN. Cerebrovascular reactivity impairment after sport-induced concussion. Med Sci Sports Exerc. 2011 Dec; 43(12):2241–8.cited 2016 Apr 22 [PubMed: 21606867]
31. Mandell DM, Han JS, Poublanc J, Crawley AP, Stainsby JA, Fisher JA, et al. Mapping cerebrovascular reactivity using blood oxygen level-dependent MRI in patients with arterial steno-occlusive disease: Comparison with arterial spin labeling MRI. Stroke. 2008; 39(7):2021–8. [PubMed: 18451352]
32. Liu P, De Vis JB, Lu H. Cerebrovascular reactivity (CVR) MRI with CO2 challenge: A technical review. Neuroimage. 2018; (March):1–12.
33. Fisher JA, Venkatraghavan L, Mikulis DJ. Magnetic Resonance Imaging–Based Cerebrovascular Reactivity and Hemodynamic Reserve. Stroke. 2018; doi: 10.1161/STROKEAHA.118.021012
34. Willie CK, Macleod DB, Shaw AD, Smith KJ, Tzeng YC, Eves ND, et al. Regional brain blood flow in man during acute changes in arterial blood gases. J Physiol. 2012; 590(14):3261–75. [PubMed: 22495584]
35. Chen JJ, Pike GB. Global cerebral oxidative metabolism during hypercapnia and hypocapnia in humans: implications for BOLD fMRI. J Cereb Blood Flow Metab. 2010; 30(6):1094–9. [PubMed: 20372169]
36. Wu CW, Gu H, Lu H, Stein EA, Chen JH, Yang Y. Mapping functional connectivity based on synchronized CMRO2 fluctuations during the resting state. Neuroimage. 2009; 45(3):694–701. [PubMed: 19280693]
37. Hoge R, Atkinson J, Gill B, Crelier G, Marrett S. Investigation of BOLD signal dependence on cerebral blood flow and oxygen consumption: The. Magn Reson Med. 1999; 863:849–63.
38. Hoge RD. Calibrated fMRI. NeuroImage. 2012; 62:930–7. [PubMed: 22369993]
39. De Vis JB, Hendrikse J, Bhogal A, Adams A, Kappelle LJ, Petersen ET. Age-related changes in brain hemodynamics; A calibrated MRI study. Hum Brain Mapp. 2015; 36(10):3973–87. [PubMed: 26177724]
40. Lajoie I, Nugent S, Debacker C, Dyson K, Tancredi FB, Badhwar AP, et al. Application of calibrated fMRI in Alzheimer's disease. NeuroImage Clin. 2017
41. De Vis JB, Petersen ET, Bhogal A, Hartkamp NS, Klijn CJM, Kappelle LJ, et al. Calibrated MRI to evaluate cerebral hemodynamics in patients with an internal carotid artery occlusion. J Cereb Blood Flow Metab. 2015

42. Cantu RC. Frequency and Location of Head Impact Exposures in Individual Collegiate Football Players. Yearb Sport Med. 2011; 2011(6):20–2.
43. Broglio SP, Surma T, Ashton-Miller JA. High school and collegiate football athlete concussions: A biomechanical review. Ann Biomed Eng. 2012; 40(1):37–46. [PubMed: 21994058]
44. Crisco JJ, Wilcox BJ, Machan JT, McAllister TW, Duhaime AC, Duma SM, et al. Magnitude of head impact exposures in individual collegiate football players. J Appl Biomech. 2012; 28(2):174–83. [PubMed: 21911854]
45. Crisco JJ, Fiore R, Beckwith JG, Chu JJ, Brolinson PG, Duma S, et al. Frequency and location of head impact exposures in individual collegiate football players. J Athl Train. 2010; 45(6):549–59. [PubMed: 21062178]
46. Clark MD, Varangis EML, Champagne AA, Giovanello KS, Shi F, Kerr ZY, et al. Effects of career duration, concussion history, and playing position on white matter microstructure and functional neural recruitment in former college and professional football athletes. Radiology. 2018; 286(3)
47. Concussion in Sport Group. Sport Concussion Assessment Tool - 3rd Edition. British Journal of Sports Medicine. 2013; 47:259. [PubMed: 23479480]
48. Slessarev M, Han J, Mardimae A, Prisman E, Preiss D, Volgyesi G, et al. Prospective targeting and control of end-tidal CO2 and O2 concentrations. J Physiol. 2007; 581(Pt 3):1207–19. [PubMed: 17446225]
49. Bulte DP, Chiarelli P a, Wise RG, Jezzard P. Cerebral perfusion response to hyperoxia. J Cereb Blood Flow Metab. 2007; 27(1):69–75. [PubMed: 16670698]
50. Willie CK, Macleod DB, Shaw AD, Smith KJ, Tzeng YC, Eves ND, et al. Regional brain blood flow in man during acute changes in arterial blood gases. J Physiol. 2012
51. Ainslie PN, Duffin J. Integration of cerebrovascular CO2 reactivity and chemoreflex control of breathing: Mechanisms of regulation, measurement, and interpretation. Am J Physiol - Regul Integr Comp Physiol. 2009; 296(5)
52. Peirce JW. Generating stimuli for neuroscience using PsychoPy. Front Neuroinform. 2008; :2.doi: 10.3389/neuro.11.010.2008 [PubMed: 18974794]
53. Peirce JW. PsychoPy-Psychophysics software in Python. J Neurosci Methods. 2007; 162(1–2):8–13. [PubMed: 17254636]
54. Alsop DC, Detre JA, Golay X, Gunther M, Hendrikse J, Hernandez-Garcia L, et al. Recommended implementation of arterial spin-labeled Perfusion mri for clinical applications: A consensus of the ISMRM Perfusion Study group and the European consortium for ASL in dementia. Magn Reson Med. 2015; 73(1):102–16. [PubMed: 24715426]
55. Wu W, Buxton RB, Wong EC. Vascular space occupancy weighted imaging with control of residual blood signal and higher contrast-to-noise ratio. IEEE Trans Med Imaging. 2007; 26(10):1319–27. [PubMed: 17948723]
56. Jenkinson M, Beckmann CF, Behrens TEJ, Woolrich MW, Smith SM. Fsl. Neuroimage. 2012; 62(2):782–90. [PubMed: 21979382]
57. Cox R. AFNI : Software for Analysis and Visualization of Functional Magnetic Resonance Neuroimages. Comput Biomed Res. 1996; 29(3):162–73. [PubMed: 8812068]
58. Jenkinson M, Bannister P, Brady M, Smith S. Improved optimization for the robust and accurate linear registration and motion correction of brain images. Neuroimage. 2002; 17(2):825–41. [PubMed: 12377157]
59. Jenkinson, Mark; Bannister, Peter. Improved Methods for the Registration and Motion Correction of Brain Images. Neuroimage. 2002; 17(2):825–41. [PubMed: 12377157]
60. Andersson JLR, Skare S, Ashburner J. How to correct susceptibility distortions in spin-echo echo-planar images: application to diffusion tensor imaging. Neuroimage. 2003 Oct; 20(2):870–88.cited 2016 Mar 1 [PubMed: 14568458]
61. Smith SM, Jenkinson M, Woolrich MW, Beckmann CF, Behrens TEJ, Johansen-berg H, et al. Advances in Functional and Structural MR Image Analysis and Implementation as FSL Technical Report TR04SS2. Neuroimage. 2004; 23(S1):208–19.
62. Smith SM, Brady JM. SUSAN—A New Approach to Low Level Image Processing. Int J Comput Vis. 1997; 23(1):45–78.

63. Wang J, Alsop DC, Song HK, Maldjian JA, Tang K, Salvucci AE, et al. Arterial transit time imaging with flow encoding arterial spin tagging (FEAST). Magn Reson Med. 2003; 50(3):599–607. [PubMed: 12939768]
64. Herscovitch P, Raichle ME. What is the correct value for the brain--blood partition coefficient for water? J Cereb Blood Flow Metab. 1985; 5(1):65–9. [PubMed: 3871783]
65. Zhang X, Petersen ET, Ghariq E, De Vis JB, Webb a G, Teeuwisse WM, et al. In vivo blood T(1) measurements at 1.5 T, 3 T, and 7 T. Magn Reson Med. 2012; :1–5. DOI: 10.1002/mrm.24550
66. Aslan S, Xu F, Wang PL, Uh J, Yezhuvath US, Van Osch M, et al. Estimation of labeling efficiency in pseudocontinuous arterial spin labeling. Magn Reson Med. 2010; 63(3):765–71. [PubMed: 20187183]
67. Germuska M, Merola A, Murphy K, Babic A, Richmond L, Khot S, et al. A forward modelling approach for the estimation of oxygen extraction fraction by calibrated fMRI. Neuroimage. 2016; 139:313–23. [PubMed: 27282477]
68. Ma, Y; Berman, AJL; Pike, GB. The Effect of Dissolved Oxygen on Relaxation Rates of Blood Plasma. Proceedings 22nd Scientific Meeting International Society for Magnetic Resonance in Medicine; 2014. 3099
69. Zhang Y, Brady M, Smith S. Segmentation of brain MR images through a hidden Markov random field model and the expectation-maximization algorithm. IEEE Trans Med Imaging. 2001; 20(1):45–57. [PubMed: 11293691]
70. Donahue MJ, Strother MK, Lindsey KP, Hocke LM, Tong Y, deB Frederick B. Time delay processing of hypercapnic fMRI allows quantitative parameterization of cerebrovascular reactivity and blood flow delays. J Cereb Blood Flow Metab. 2016; 36:1767–79. [PubMed: 26661192]
71. Duffin J, Sobczyk O, Crawley AP, Poublanc J, Mikulis DJ, Fisher JA. The dynamics of cerebrovascular reactivity shown with transfer function analysis. Neuroimage. 2015; 114:207–16. [PubMed: 25891374]
72. Poublanc J, Crawley AP, Sobczyk O, Montandon G, Sam K, Mandell DM, et al. Measuring cerebrovascular reactivity: the dynamic response to a step hypercapnic stimulus. J Cereb Blood Flow Metab. 2015; (April):1–11. DOI: 10.1038/jcbfm.2015.114 [PubMed: 25352045]
73. Champagne AA, Bhogal AA, Coverdale NS, Mark CI, Cook DJ. A novel perspective to calibrate temporal delays in cerebrovascular reactivity using hypercapnic and hyperoxic respiratory challenges. Neuroimage. 2017; 11(044)
74. Davis TL, Kwong KK, Weisskoff RM, Rosen BR. Calibrated functional MRI: mapping the dynamics of oxidative metabolism. Proc Natl Acad Sci U S A. 1998; 95(4):1834–9. [PubMed: 9465103]
75. Gauthier CJ, Desjardins-Crépeau L, Madjar C, Bherer L, Hoge RD. Absolute quantification of resting oxygen metabolism and metabolic reactivity during functional activation using QUO2 MRI. Neuroimage. 2012; 63(3):1353–63. [PubMed: 22986357]
76. Gauthier CJ, Hoge RD. Magnetic resonance imaging of resting OEF and CMRO2 using a generalized calibration model for hypercapnia and hyperoxia. Neuroimage. 2012; 60(2):1212–25. [PubMed: 22227047]
77. Boxerman JL, Hamberg LM, Rosen BR, Weisskoff RM. Mr contrast due to intravascular magnetic susceptibility perturbations. Magn Reson Med. 1995; 34(4):555–66. [PubMed: 8524024]
78. Blockley NP, Griffeth VEM, Germuska MA, Bulte DP, Buxton RB. An analysis of the use of hyperoxia for measuring venous cerebral blood volume: Comparison of the existing method with a new analysis approach. Neuroimage. 2013; 72:33–40. [PubMed: 23370053]
79. Bulte D, Chiarelli P, Wise RG, Jezzard P. Measurement of cerebral blood volume in humans using hyperoxic MRI contrast. J Magn Reson Imaging. 2007; 26(4):894–9. [PubMed: 17896390]
80. Andersson JLR, Jenkinson M, Smith S. Non-linear registration aka Spatial normalisation FMRIB Technial Report TR07JA2. In Pract. 2007; (June):22.
81. Chen G, Adleman NE, Saad ZS, Leibenluft E, Cox RW. Applications of multivariate modeling to neuroimaging group analysis: A comprehensive alternative to univariate general linear model. Neuroimage. 2014
82. Cox RW, Reynolds RC, Taylor PA. AFNI and Clustering: False Positive Rates Redux. bioRxiv. 2016

83. Cox RW, Chen G, Glen DR, Reynolds RC, Taylor PA. FMRI Clustering in AFNI: False-Positive Rates Redux. Brain Connect. 2017; 7(3):152–71. [PubMed: 28398812]
84. Boxerman JL, Bandettini PA, Kwong KK, Baker JR, Davis TL, Rosen BR, et al. The Intravascular Contribution to fMRI Signal Change: Monte Carlo Modeling and Diffusion-Weighted Studies in Vivo.
85. Mazziotta J, Toga A, Evans A, Fox P, Lancaster J, Zilles K, et al. A probabilistic atlas and reference system for the human brain: International Consortium for Brain Mapping (ICBM). Philos Trans R Soc London B Biol Sci. 2001; 356(1412):1293–322. [PubMed: 11545704]
86. Ellis MJ, Ryner LN, Sobczyk O, Fierstra J, Mikulis DJ, Fisher JA, et al. Neuroimaging Assessment of Cerebrovascular Reactivity in Concussion: Current Concepts, Methodological Considerations, and Review of the Literature. Front Neurol. 2016; 7(April):1–16. DOI: 10.3389/fneur.2016.00061/abstract [PubMed: 26834696]
87. Corps KN, Roth TL, McGavern DB. Inflammation and neuroprotection in traumatic brain injury. JAMA Neurol. 2015; 72(3):355–62. [PubMed: 25599342]
88. Hinson HE, Rowell S, Schreiber M. Clinical evidence of inflammation driving secondary brain injury: a systematic review. J Trauma Acute Care Surg. 2015; 78(1):184–91. [PubMed: 25539220]
89. Halani S, Kwinta JB, Golestani AM, Khatamian YB, Chen JJ. Comparing cerebrovascular reactivity measured using BOLD and cerebral blood flow MRI: The effect of basal vascular tension on vasodilatory and vasoconstrictive reactivity. Neuroimage. 2015; 110:110–23. DOI: 10.1016/j.neuroimage.2015.01.050 [PubMed: 25655446]
90. Fierstra J, Poublanc J, Han JS, Silver F, Tymianski M, Crawley AP, et al. Steal physiology is spatially associated with cortical thinning. J Neurol Neurosurg Psychiatry. 2010; 81(3):290–3. [PubMed: 20185465]
91. Tremblay S, De Beaumont L, Henry LC, Boulanger Y, Evans AC, Bourgouin P, et al. Sports Concussions and Aging: A Neuroimaging Investigation. Cereb Cortex. 2013; 23(5):1159–66. DOI: 10.1093/cercor/bhs102 [PubMed: 22581847]
92. Liu P, Hebrank AC, Rodrigue KM, Kennedy KM, Park DC, Lu H. A comparison of physiologic modulators of fMRI signals. Hum Brain Mapp. 2013; 34(9):2078–88. [PubMed: 22461234]
93. Len TK, Neary JP, Asmundson GJG, Goodman DG, Bjornson B, Bhambhani YN. Cerebrovascular reactivity impairment after sport-induced concussion. Med Sci Sports Exerc. 2011; 43(12):2241–8. [PubMed: 21606867]
94. Wojtowicz M, Iverson GL, Silverberg ND, Mannix R, Zafonte R, Maxwell B, et al. Consistency of Self-Reported Concussion History in Adolescent Athletes. J Neurotrauma. 2016
95. Meehan WP, Mannix RC, Oebrien MJ, Collins MW. The prevalence of undiagnosed concussions in athletes. Clin J Sport Med. 2013
96. Wallace J, Covassin T, Nogle S, Gould D, Kovan J. Knowledge of Concussion and Reporting Behaviors in High School Athletes With or Without Access to an Athletic Trainer. J Athl Train. 2017
97. Para AE, Sam K, Poublanc J, Fisher JA, Crawley AP, Mikulis DJ. Invalidation of fMRI experiments secondary to neurovascular uncoupling in patients with cerebrovascular disease. J Magn Reson Imaging. 2017
98. van Niftrik CHB, Piccirelli M, Bozinov O, Maldaner N, Strittmatter C, Pangalu A, et al. Impact of baseline CO2on Blood-Oxygenation-Level-Dependent MRI measurements of cerebrovascular reactivity and task-evoked signal activation. Magn Reson Imaging. 2018

Europe PMC Funders Author Manuscripts

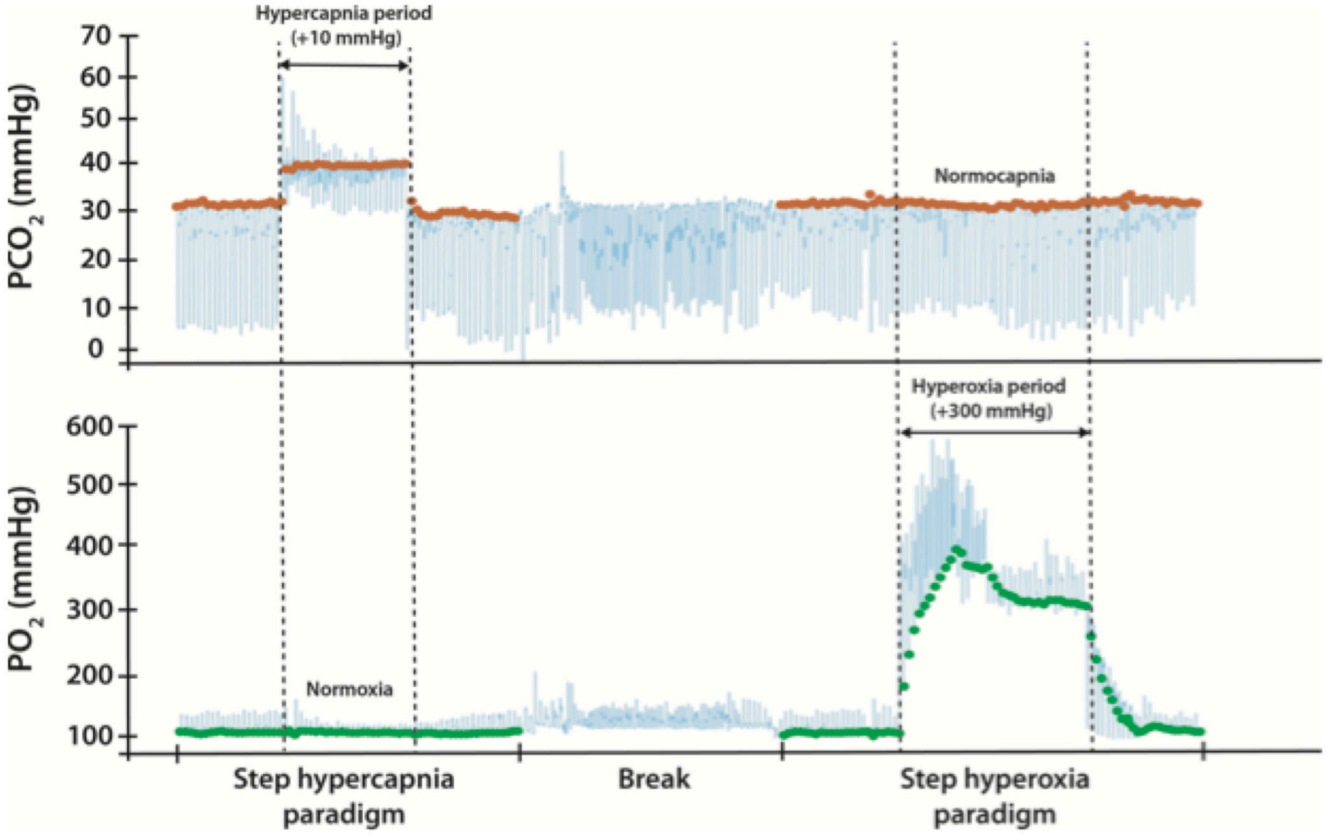

Figure 1. Examples of $P_{ET}CO_2$ and $P_{ET}O_2$ traces from the respiratory manipulations in a single representative participant

The continuous traces (blue) for P_{CO2} (top) and P_{O2} (bottom) sampled from the computerized RA-MR™ (Thornhill Research Inc., Toronto, ON) apparatus during the hypercapnic and hyperoxic breathing protocols. End-tidal values are indicated for CO_2 (red filled circles) and O_2 (green filled circles).

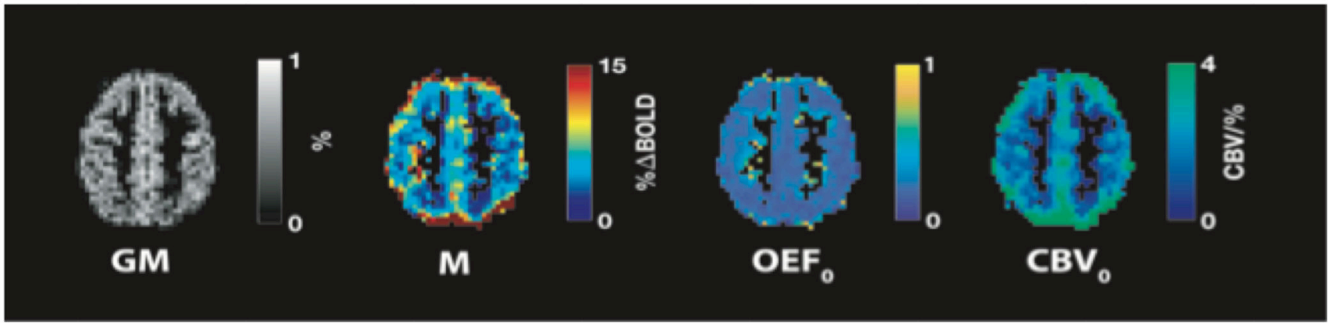

Figure 2. Sample grey-matter (GM) maps of M, resting oxygen extraction fraction (OEF_O) and cerebral blood volume (CBV_O) in an individual subject

Europe PMC Funders Author Manuscripts

Europe PMC Funders Author Manuscripts

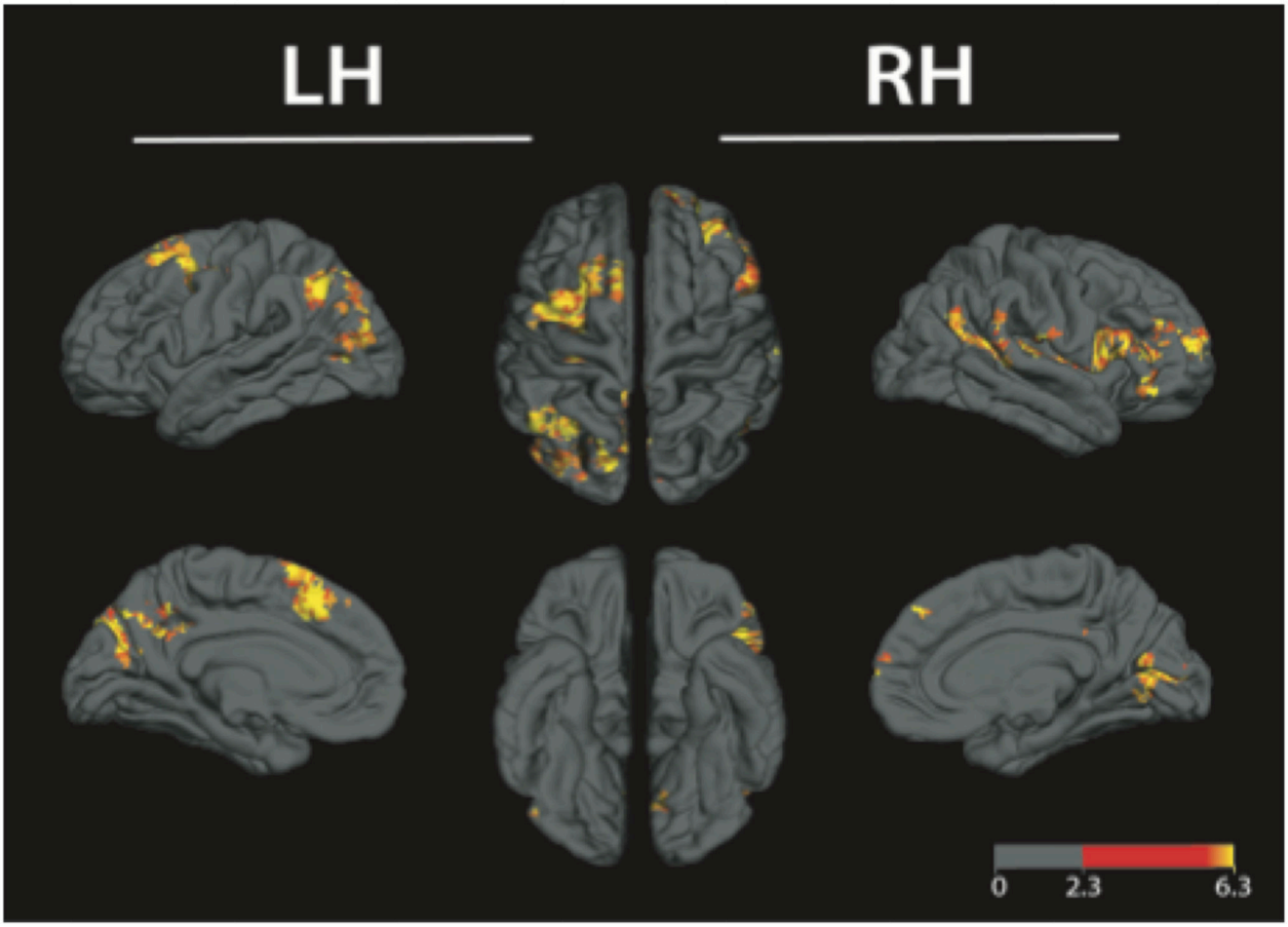

Figure 3. BOLD-CVR statistical results from the voxelwise group analysis between subjects with and without a history of concussion

Regions in yellow-orange show significantly increased BOLD-CVR in the HX group compared to the CTL subjects. Image corrected for multiple comparisons at $P < 0.05$, and dilated on the freesurfer template (https://surfer.nmr.mgh.harvard.edu) for visual purposes. LH = left hemisphere, RH = right hemisphere

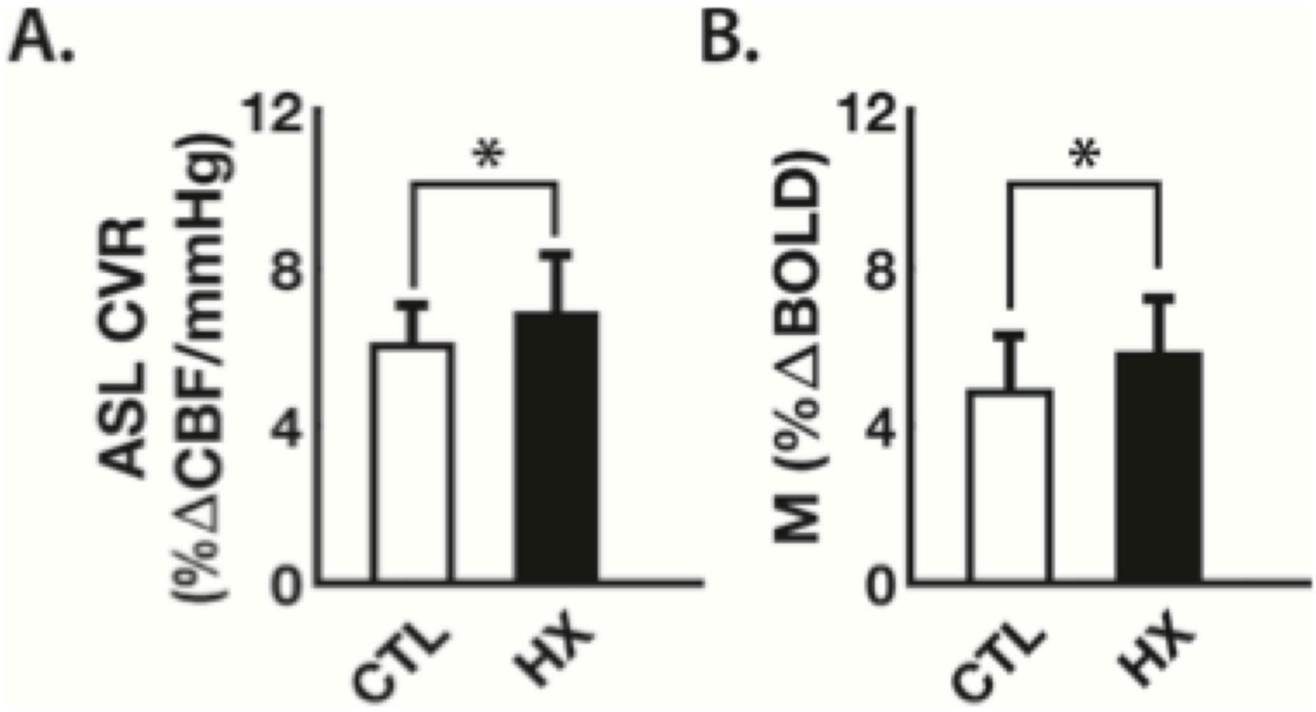

Figure 4. Bar plots of regional vascular and hemodynamic parameters tested *post-hoc* between the groups

Values represent the mean ± standard deviation parameters extracted from the region of interest highlighted in Fig. 3. White bar plots represent the control group (CTL, no history of concussion), while black bars represent players with previous history of head injury (HX). Group parameters were tested using an ANCOVA with height, weight, age and resting end-tidal CO_2 values as covariates. ASL CVR = arterial spin labelling cerebrovascular reactivity, BOLD = blood oxygen level dependent, CBF = cerebral blood flow

Europe PMC Funders Author Manuscripts

Europe PMC Funders Author Manuscripts

Table 1

Demographics

	CTL (N = 31)	HX (N = 32)	*P-value* *
Age (years)	19 ± 2	19 ± 3	0.713
Height (cm)	183 ± 10	182 ± 10	0.763
Weight (kg)	99 ± 17	95 ± 13	0.357
Number of prior concussions	0	2 ± 1 (range: 1-4)	**< 0.00001**
Time since injury (years)	N/A	3.46 ±2.70 (range: 1-9)	N/A
SCAT symptom score (/ 22)	1 ± 1	4 ± 5	**0.005**
SCAT severity score (/132)	1 ± 3	7 ± 12	**0.013**

* Statistically compared using a univariate ANOVA. Values are mean ± standard deviation. N/A = not applicable, SCAT = sport-concussion assessment tool, SRC = sport-related concussion

Europe PMC Funders Author Manuscripts

Table 2
Summary of parametrization for proposed variables of interest

Parallel parameters	Imaging paradigm	Physiological interpretation on BOLD-CVR
ASL-CVR	Hypercapnia pCASL	Dynamic vascular effect
CBV_0	Hyperoxia pCASL	Static vascular effect
OEF_0		Resting metabolic effect
κ^*	Dual-calibration with both paradigms	Lumped parameter for [Hb], vessel size and morphology, and other intra- and extra-vascular effects

*κ was computed using ***Eq.* (3)** where β was set to 1.3 (84). ASL = arterial spin labelling, BOLD = blood oxygen level dependent, CVR = cerebrovascular reactivity, CBV_0 = resting cerebral volume, OEF_0 = oxygen extraction fraction, pCASL = pseudo-continuous arterial spin labelling

Europe PMC Funders Author Manuscripts

Table 3
End-tidal measurements during respiratory protocols

	Mean ± standard deviation		*P*-value*
	CTL (N = 31)	HX (N = 32)	
Hypercapnia			
Baseline $P_{ET}CO_2$ (mmHg)	42 ±3	40 ±4	0.078
Baseline $P_{ET}O_2$ (mmHg)	109 ±6	108 ±4	0.209
Δ $P_{ET}CO_2$ (mmHg)	8 ±2	8 ±2	0.107
Δ $P_{ET}O_2$ (mmHg)	3 ± 3	3 ± 4	0.651
Hyperoxia			
Baseline $P_{ET}CO_2$ (mmHg)	110 ± 8	108 ±5	0.061
Baseline $P_{ET}O_2$ (mmHg)	41 ±3	39 ±5	0.117
Δ $P_{ET}CO_2$ (mmHg)	0 ± 1	0 ± 1	0.215
Δ $P_{ET}O_2$ (mmHg)	233 ±37	229 ± 48	0.695

*Statistically compared using a univariate ANOVA. $P_{ET}O_2$ = partial pressure of end-tidal carbon dioxide, $P_{ET}O_2$ = partial pressure of end-tidal oxygen

Table 4

Significant clusters from BOLD-CVR group-analysis between subjects with and without a history of concussion.

Cluster	Size (Voxels)	Center of mass (mm)*			Peak*			Location (focus point)
		X	Y	Z	X	Y	Z	
1	1571	46.1	5.4	12.4	66.7	-41.4	2.2	right precentral gyrus, central and frontal opercular cortices left lateral occipital
2	1440	-22.9	-71.4	32.6	-50.5	-63.9	42.3	cortex, cuneal cortex, precuneus cortex
3	910	-20.6	7.7	57.6	-6.1	24.5	49.2	right superior and middle frontal gyrus

*Coordinates were converted from Talairach space to the Montreal Neurological Institute template and identified using the *3Dclust and whereami* functions in AFNI (66). Clusters were threshold at $P < 0.05$ and size > 602 voxels

Europe PMC Funders Author Manuscripts

Table 5
Summary of parametrization for proposed variables of interest

Parameters	Unstandardized beta	Standard error	Wald	Standardized beta [a]	*P*-values
ASL-CVR	1.0	0.4	8.6	0.4	0.003
CBV_0	4.4	1.5	9.4	0.6	0.002
OEF_0	28.1	8.3	11.6	0.8	0.001
κ^*	0.4	0.1	8.2	0.7	0.004

[*] κ was computed using ***Eq.* (3)** where β was set to 1.3 (84).

[a] coefficients were standardized using Hoerger logistic regression standardization (93). ASL = arterial spin labelling, BOLD = blood oxygen level dependent, CVR = cerebrovascular reactivity, CBV_0 = resting cerebral volume, OEF_0 = oxygen extraction fraction, pCASL = pseudo-continuous arterial spin labelling